

Polarization studies of H(2p) charge-exchange excitation: H⁺-He collisions

R. Hippler, M. Faust, R. Wolf,* H. Kleinpoppen,[†] and H. O. Lutz

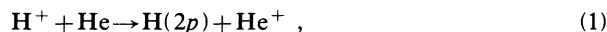
Fakultät für Physik, Universität Bielefeld, D-4800 Bielefeld, Federal Republic of Germany

(Received 28 May 1987)

Alignment and orientation for H(2p) excitation in H⁺-He collisions have been measured for incident proton energies of 1–4 keV, and scattering angles between 0.5° and 3.5°. From the results the relative population of magnetic substates H(2p₀) and H(2p_{±1}) (i.e., the differential alignment and orientation) is extracted. The results are in excellent agreement with recent theoretical calculations. The observed magnitude of H(2p₀) excitation demonstrates that, in addition to a 2pσ-2pπ rotational coupling, a 2pσ-2sσ radial coupling is effective at small impact parameters.

I. INTRODUCTION

Charge-changing collisions involving simply structured ion-atom collision systems are of considerable basic as well as applied interest. Advances in experiment as well as in theory have made it possible to unveil very subtle details of such processes. In two earlier papers^{1,2} we have investigated charge-exchange excitation in H⁺+Ar→H(2p)+Ar⁺ collisions, whereby information about H(2p) was extracted performing a photon-scattered projectile coincidence measurement. While providing a detailed analysis of the underlying collision mechanism, this experiment was, however, from a basic point of view, not ideal. The remaining Ar⁺ ion is left in an ensemble of states |l, m_l⟩ whose relative population is not known, and part of the information contained in the collision is thus not available. We have now investigated the collision system,



at low incident velocities where the He⁺ ion is predominantly left in its ground state. Therefore, this fundamental two-electron system can be characterized completely in a quantum-mechanical sense.^{3–5} In addition, it is of considerable theoretical interest since electron-electron interaction during the collision is not negligible. Theoretical calculations, which include this type of interaction are now available^{6,7} and will be compared with the present data.

Angular correlation and polarization studies of ion-atom collisions have proven to yield detailed information about the underlying collision mechanisms (see, e.g., Ref. 5). In particular, such measurements provide information about nonuniform population of magnetic substates |m⟩ and allow us to derive magnitude and relative phase of scattering amplitudes. More formally, this information may be expressed in terms of multipole moments, commonly referred to as orientation and alignment.^{4,8} To extract alignment and orientation we use the scattered projectile-polarized photon coincidence technique, i.e., we perform a (linear and circular) polarization analysis of light emitted during the decay of the excited H(2p) state to the H(1s) ground state in coin-

idence with the detection of projectiles scattered through selected scattering angles θ_s. Introducing scattering amplitudes f_m with m referring to the z component of the orbital angular momentum of H(2p), one may express the monopole ⟨T(1)₀₀⟩ and the spin-averaged components of the orientation vector ⟨T(1)₁₁⟩ and of the alignment tensor ⟨T(1)_{2Q}⟩ (Q=0,1,2) as⁴

$$\begin{aligned} \langle T(1)_{00} \rangle &= \sigma(2p) / \sqrt{3}, \\ \langle T(1)_{11} \rangle &= -i\sqrt{2} \text{Im}[f_1 f_0^*], \\ \langle T(1)_{20} \rangle &= \sqrt{2/3} (|f_1|^2 - |f_0|^2), \\ \langle T(1)_{21} \rangle &= -\sqrt{2} \text{Re}[f_1 f_0^*], \\ \langle T(1)_{22} \rangle &= f_1 f_{-1}^*, \end{aligned} \quad (2)$$

with σ(2p)=Σ_mσ_m the differential scattering cross section for H(2p) charge-exchange excitation, and σ_m=|f_m|² the partial cross section. The orientation vector is related to the y component of the transferred angular momentum L via

$$i \langle T(1)_{11} \rangle / \langle T(1)_{00} \rangle = -(\sqrt{3}/2) \langle L_y \rangle.$$

Here we have used a right-handed coordinate frame with the z axis along the direction of the incident projectile, the direction of the outgoing projectile lying in the x-z (scattering) plane, and with the y axis perpendicular to the scattering plane. The degrees of linear and circular polarization (Stokes parameters⁹) are given by

$$\begin{aligned} P_1 &= [I(0^\circ) - I(90^\circ)] / [I(0^\circ) + I(90^\circ)], \\ P_2 &= [I(45^\circ) - I(135^\circ)] / [I(45^\circ) + I(135^\circ)], \\ P_3 &= [I(-) - I(+)] / [I(+) + I(-)]. \end{aligned} \quad (3)$$

I(β) is the intensity transmitted by a linear polarizer, with β the angle between the plane of polarization and the z axis. I(+) and I(-) denote the intensity of circularly polarized light with positive and negative helicity, respectively. The Stokes parameters depend on the collision-induced alignment and orientation; for the experimental situation chosen here (observation angle θ_γ=90°) we have

$$\begin{aligned}
 P_1 &= -[\langle T(1)_{22} \rangle \cos(2\phi) + \sqrt{3/2} \langle T(1)_{20} \rangle] / I, \\
 P_2 &= 2 \langle T(1)_{21} \rangle \sin(\phi) / I, \\
 P_3 &= (\frac{14}{3}) i \langle T(1)_{11} \rangle \sin(\phi) / I, \\
 I &= 2\sqrt{3} \langle T(1)_{00} \rangle + \langle T(1)_{22} \rangle \cos(2\phi) - 1/\sqrt{6} \langle T(1)_{20} \rangle,
 \end{aligned}
 \tag{4}$$

where ϕ is the azimuthal angle of the photon detection relative to the scattering plane. Equations (4) take into account the depolarization caused by the spin-orbit interaction; the hyperfine interaction is weak in hydrogen and was neglected. The total polarization P , corrected for fine-structure coupling, is given by¹⁰

$$P^2 = (\frac{7}{3})^2 P_1^2 + (\frac{7}{3})^2 P_2^2 + P_3^2. \tag{5}$$

In case the collision produces a quantum-mechanical pure state (i.e., in case of complete coherence) we have $P=1$.

II. EXPERIMENTAL METHOD

The experimental arrangement has been described previously in some detail.² Basically, protons with kinetic energies of a few keV enter a scattering chamber through suitably chosen diaphragms reducing its diameter to about 2 mm. After hitting a thermal helium-gas target the beam is collected 300–1200 mm (depending on the scattering angles chosen) downstream in two concentric Faraday cups having diameters of 3 and 6 mm, respectively. Typically, more than 95% of the beam intensity is collected in the inner cup.

Fast neutralized projectiles scattered through selected scattering angles are detected in a position-sensitive detector consisting of two microchannel plates and an anode array. The anode array is composed of 32 individual electrodes and covers eight azimuthal angles ϕ for each of four scattering angles θ_s . Pulses from the 32 anodes are processed separately; they serve as start inputs for 32 time-to-digital converters (TDC).

Photons produced in the collision region are detected with a photomultiplier (EMR 542J) having a LiF window and a KBr photocathode. The photomultiplier views the interaction region at $\theta_\gamma = 90^\circ$ through a polarization-sensitive device. This consists of a plane LiF mirror positioned at Brewster's angle (about 60°) with respect to the photon direction. It is mounted on a turntable to allow rotation about its optical axis which is necessary for polarization measurements. The instrumental polarization of this arrangement was measured to be 90%. A quarter-wave plate made of MgF₂ was used for the circular polarization measurements. The instrumental (circular) polarization of the $\lambda/4$ plate was measured to be 99%. The effect of the final angular resolution has been taken into account; the measured polarizations have been corrected accordingly. Pulses from the Lyman- α photomultiplier were suitably delayed and served as stop inputs for the TDC system. Data processing is performed by a LSI 11/23 microprocessor, which also controls the experiment.

III. RESULTS

In Fig. 1, a typical set of polarization measurements is presented. The data were measured simultaneously for the eight azimuthal angles ϕ shown. The orientation vector and the three components of the alignment tensor

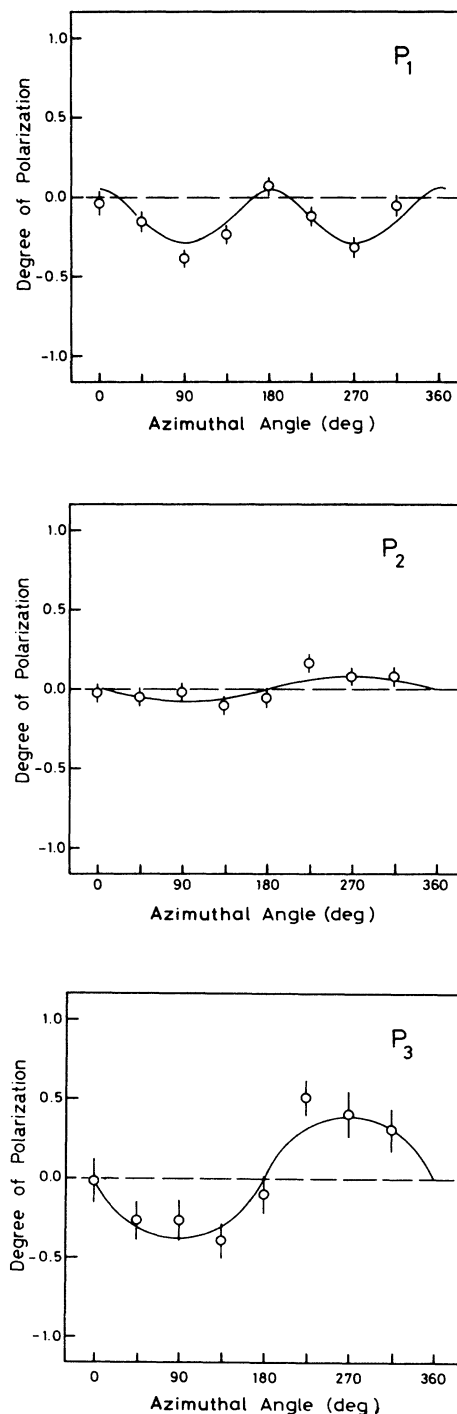


FIG. 1. Degree of polarization vs azimuthal angle ϕ for 1.5-keV H⁺-He collisions and scattering angle $\theta_s = 1.4^\circ$. The two linear (P_1, P_2) and the circular (P_3) polarizations are shown.

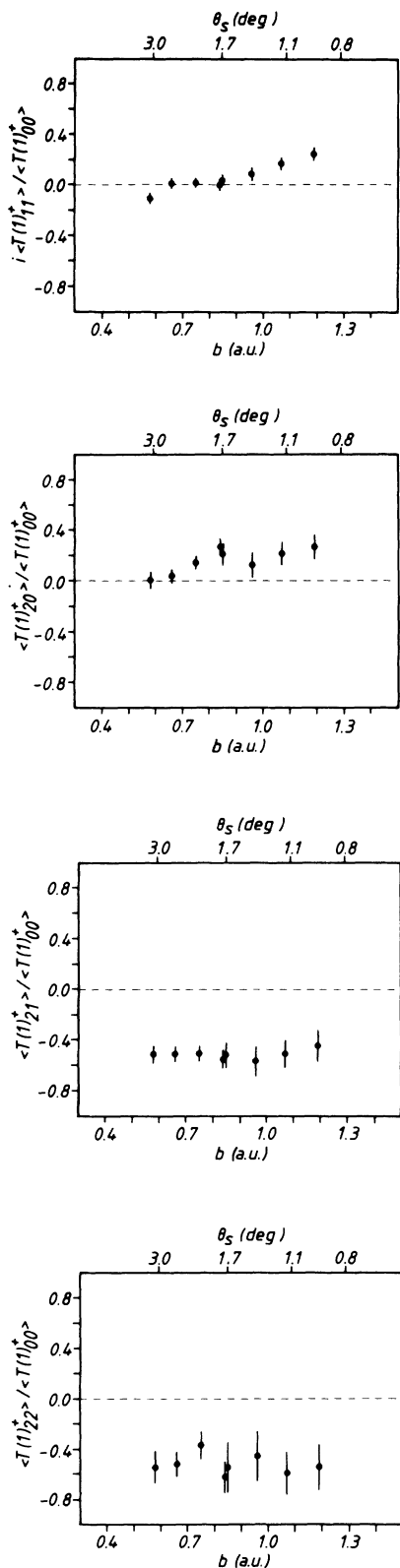


FIG. 2. Relative orientation vector $\langle T(1)_{11} \rangle / \langle T(1)_{00} \rangle$ and alignment tensor components $\langle T(1)_{2Q} \rangle / \langle T(1)_{00} \rangle$ ($Q=0,1,2$) vs impact parameter b for 1-keV H^+ -He collisions. θ_s is the scattering angle of the projectile.

are obtained from such data by least-squares fits to Eqs. (4).

Figures 2–5 display the relative orientation vector $i \langle T(1)_{11} \rangle / \langle T(1)_{00} \rangle$ and the three components of the alignment tensor $\langle T(1)_{2Q} \rangle / \langle T(1)_{00} \rangle$ ($Q=0,1,2$) for 1-, 1.5-, 3-, and 4-keV H^+ impact, respectively, and for

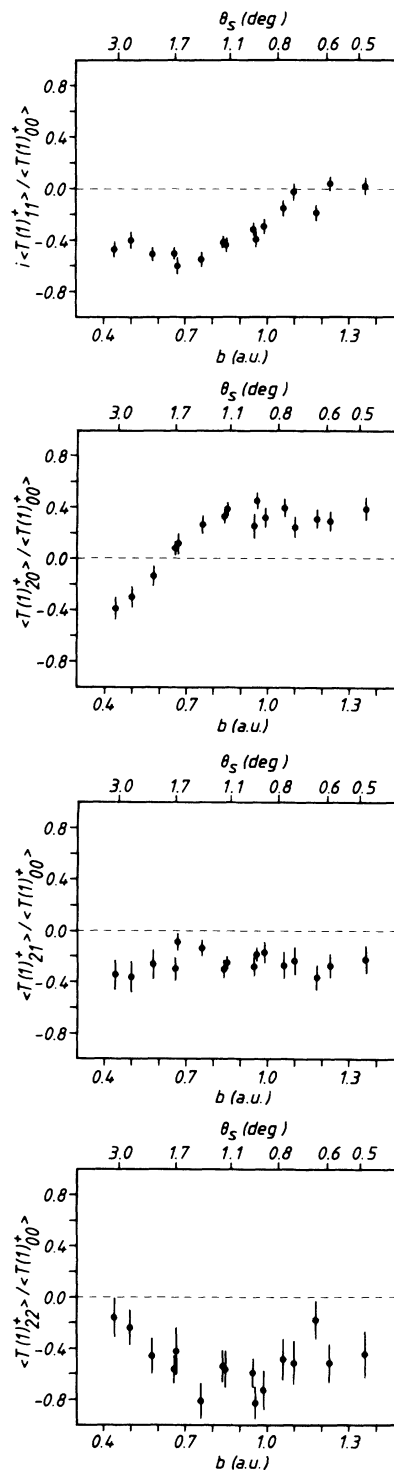


FIG. 3. Same as Fig. 2, but for 1.5-keV H^+ -He collisions.

scattering angles in the range of about 0.5° – 3.5° . The full range of impact parameters b covered in the 1–4-keV measurements lies between 0.2 and 1.3 a.u. Transformation of scattering angles θ_s to impact parameters was done by applying a Moliere potential (see, e.g., Ref. 11).

The total polarization P [Eq. (5)] measured perpendicular to the scattering plane is displayed in Fig. 6. Typically, P amounts to about 70–80% at 1 and 1.5 keV and to about 60% at 3 and 4 keV. Thus, P is significantly smaller than unity. There are two experimental reasons which could produce such a depolarization. At low in-

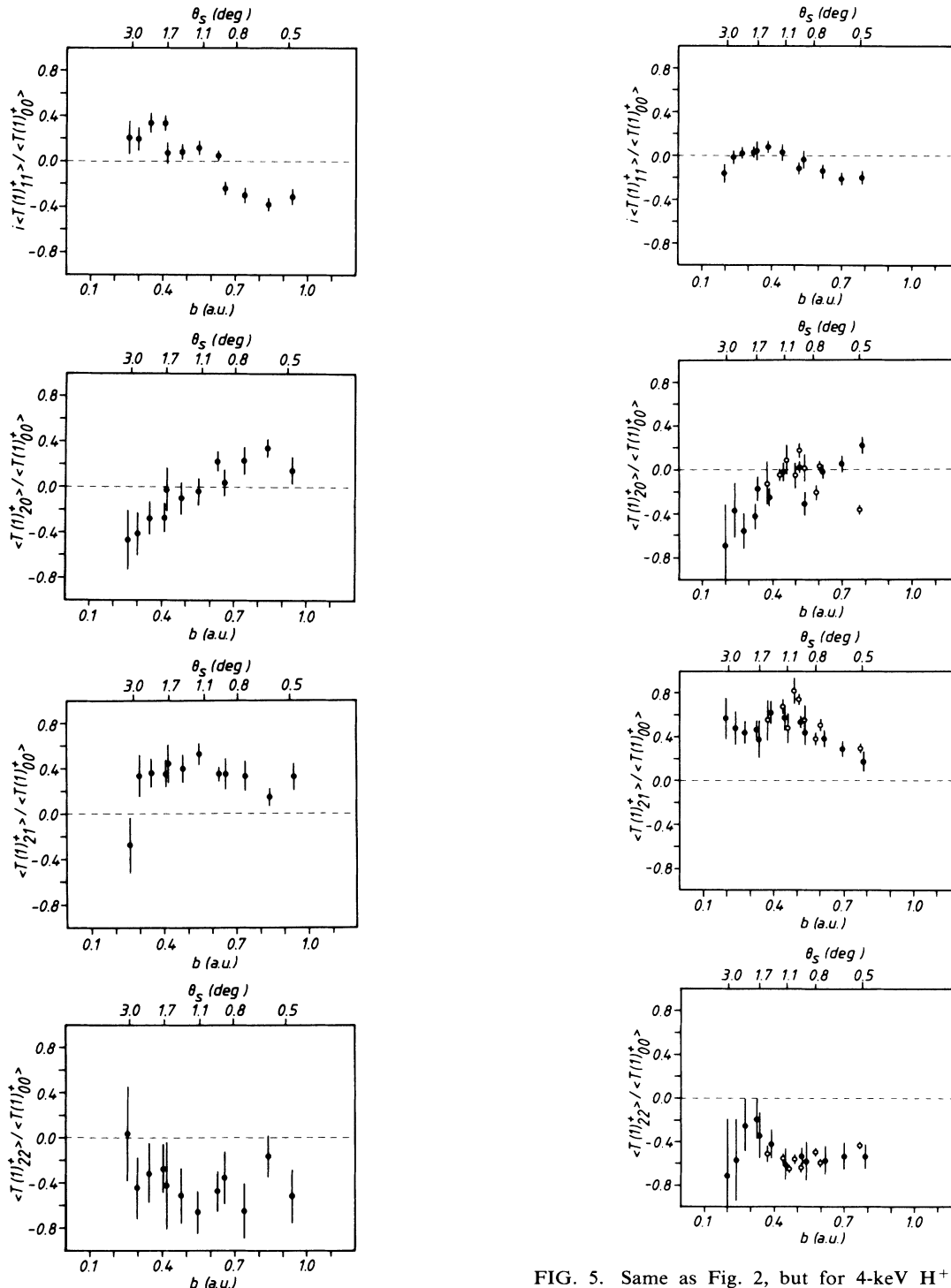


FIG. 4. Same as Fig. 2, but for 3-keV H^+ -He collisions.

FIG. 5. Same as Fig. 2, but for 4-keV H^+ -He collisions. The present results (closed circles) are compared with results from Mueller and Jaecks (Ref. 11) (open circles).

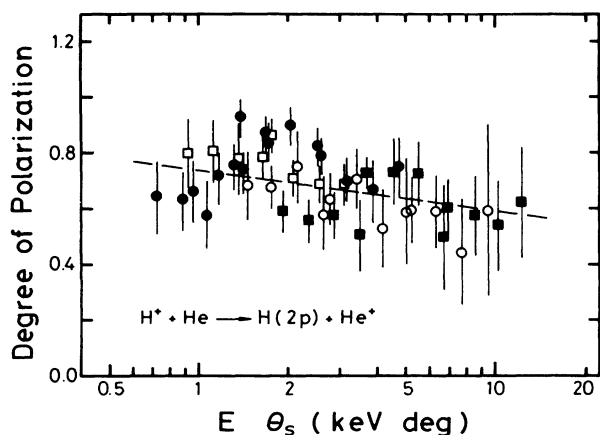


FIG. 6. Total polarization P perpendicular to the scattering plane vs projectile energy times scattering angle, $E\theta_s$, for 1 (\square), 1.5 (\bullet), 3 (\circ), 4 (\blacksquare)-keV H^+ -He collisions.

cident energies around 1 keV the total cross sections for $H(2p)$ production in H^+ -He collisions are about a factor of 200 smaller than in H -He collisions (see, e.g., Ref. 12). This implies that even with a neutral hydrogen atom, contamination of the proton beam at the 10^{-3} level H -He collisions could contribute as much as 20% to the measured signal rate.

In addition, depolarization may be caused by cascading transitions¹³ and by simultaneous excitation of both target and projectile.¹⁴ Both effects are expected to become significant at larger incident energies, while at low incident velocities (corresponding to proton energies of less than 1 keV) they are virtually absent.¹⁵ $H(3s)$ and $H(3d)$ excitation, for example, are expected to provide the dominant contributions for cascading transitions into $H(2p)$. However, due to an $H(3s)$ lifetime of 158 ns cascading transitions from $H(3s)$ will to a large extent decay outside the observation region seen by the $Ly-\alpha$ photomultiplier. Also, simultaneous excitation of $H(2p)$ and, for example, $He^+(n=2)$ could cause depolarization. There is some evidence from Fig. 6 that the total polarization decreases for more violent collisions. The dashed line in Fig. 6 in fact suggests that P decreases from about 75% to less than 60% when going from "soft" (small values of $E\theta_s$) to "violent" (large values of $E\theta_s$) collisions. Similar arguments have been used by Andersen *et al.*¹⁴ for $Li(2p)$ excitation in Li^+ -He collisions.

Also shown in Fig. 5 are the results of linear polarization measurements of Mueller and Jaacks,¹¹ which agree satisfactorily with our data. No circular polarization measurements have been reported by these authors. In analyzing their data Mueller and Jaacks have assumed full coherence, i.e., $P=1$, in which case a three-parameter description, for example, σ , λ , χ , for the collision process would be sufficient. However, as can be concluded from Fig. 6, this assumption is not really justified; particularly for an incident proton energy of 4 keV the total polarization amounts to about 60% only.

IV. DISCUSSION

In a quasimolecular picture of the collision process,¹⁶ $H(2p)$ excitation is expected to take place in two stages, connecting first the quasimolecular ($1s\sigma$) ground state with the next lowest ($2p\sigma$) state (Fig. 7); then the $2p\sigma$ state interacts via radial (for example, $2p\sigma-2s\sigma$ or $2p\sigma-3p\sigma$) and rotational ($2p\sigma-2p\pi$) couplings with states leading to $H(2p)$ excitation. The significance of the different couplings can be illuminated by closer inspection of the magnetic subshell populations. In Fig. 8 the relative population of $H(2p_0)$, measured with respect to the z axis, is plotted versus impact parameter. Defining

$$\lambda \equiv |f_0|^2 / (|f_0|^2 + 2|f_1|^2) = \sigma_0 / \sigma(2p)$$

we obtain

$$\lambda = (1 - \sqrt{2} \langle T(1)_{20} \rangle / \langle T(1)_{00} \rangle) / 3$$

using Eqs. (2). Obviously, $H(2p_0)$ population is relatively small at large impact parameters, whereas its contribution becomes dominant for impact parameters $b \leq 0.3$ a.u. This experimental result is in excellent agreement with theoretical calculations by Macek and Wang¹⁷ and model calculations by Fritsch.¹⁸ A physical interpretation of this result was recently given by Macek and Wang.¹⁷ Expressing the diabatic $2s\sigma$ and $2p\sigma$ molecular orbital (MO) in terms of adiabatic states Σ_2 and Σ_3 (with Σ_1 corresponding to $1s\sigma$, the quasimolecular ground state, and Σ_2 and Σ_3 the next two lowest states), they obtain

$$|2s\sigma\rangle = 0.2|\Sigma_2\rangle + 0.98|\Sigma_3\rangle,$$

$$|2p\sigma\rangle = -0.98|\Sigma_2\rangle + 0.2|\Sigma_3\rangle,$$

for internuclear separations $R \geq 0.6$ a.u. This "mixing"

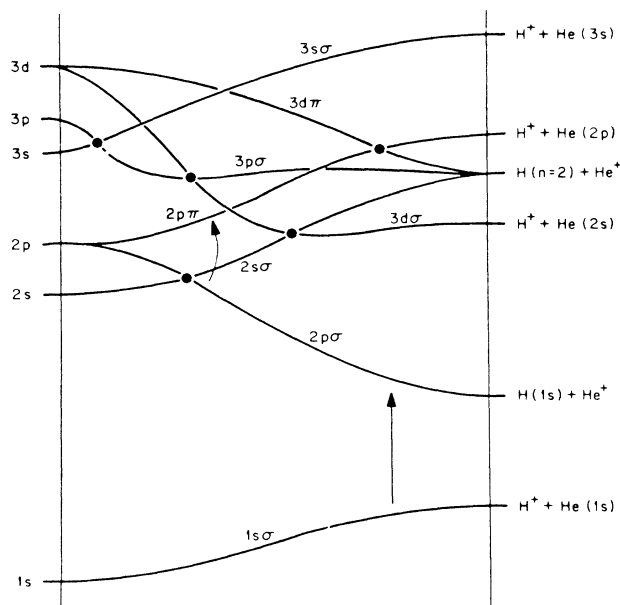


FIG. 7. Schematic correlation diagram for $(H-He)^+$ [after Macias *et al.* (Ref. 17)].

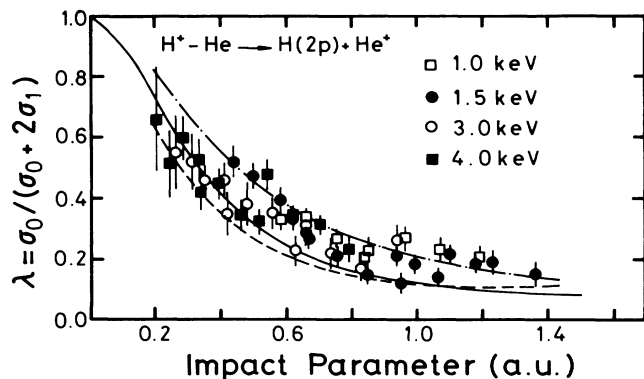


FIG. 8. Relative population of H(2p₀) vs impact parameter b for 1 (□), 1.5 (●), 3 (○), and 4 (■)-keV H⁺-He collisions. The theoretical calculation of Macek and Wang (Ref. 17) for 2.25 keV (solid line) and model calculation of Fritsch (Ref. 18) for 1 keV (dashed line) and 4 keV (dashed-dotted line) are also shown.

of states is caused by the $2p\sigma$ - $2s\sigma$ radial coupling at $R \approx 0.4$ a.u.; it means that even for $R \rightarrow \infty$, the diabatic $2s\sigma$ ($2p\sigma$) state does not converge to the adiabatic Σ_3 (Σ_2) state completely. Rotational coupling among $2p\sigma$ - $2p\pi$ hence not only populates the adiabatic Π_1 state (corresponding to the diabatic $2p\pi$), but also Σ_3 via the two-step process Σ_2 - Π_1 - Σ_3 . This two-step rotational coupling is of particular importance at small impact parameters b , whereas the one-step rotational coupling is zero for $b = 0$ and has a maximum around $b \approx 1$ a.u.

While the agreement of these calculations with our impact-parameter-dependent results appears to be excellent, this does not hold for the integral alignment $A_{20} = (\sigma_1 - \sigma_0) / (\sigma_0 + 2\sigma_1)$ which was measured to be $A_{20} \approx 0$ in the energy range 1–5 keV (e.g., Ref. 19). In contrast, the above calculations result in $A_{20} \approx 0.4$, significantly larger than experiment. In fact, a closer inspection of Fig. 8 reveals that our results for λ lie, for large impact parameters $b \geq 0.6$ a.u., above the theoretical results of Macek and Wang.¹⁷ Part of this discrepancy may be resolved if one realizes that $2p\pi$ excitation via $2p\pi$ and $3d\pi$ radial coupling at large internuclear separations ($R \approx 14$ a.u.) not only results in H(2p₁) but also in He(2¹P₁) excitation. Calculations by Fayeton *et al.*¹⁵ and Kimura and Lin⁶ show that H(2p) and He(2¹P) excitation may be of comparable magnitude. Thus, only a fraction of the flux in $2p\pi$ goes to H(2p₁), and the σ_1 as calculated by Macek and Wang¹⁷ has to be reduced accordingly. In addition, other couplings, for example $2s\sigma$ - $3p\sigma$ may also contribute to H(2p₀) excitation. Also, decoupling of the electronic angular momentum from the internuclear axis at large separations^{20,21} may lead to an increased population of H(2p₀) with increasing impact parameters. Using Eq. (23) in Ref. 20 we estimate this increase of the relative population of H(2p₀) to amount to about 0.017 and 0.034 at $b = 1$ a.u. and for 1 and 4 keV incident energy, respectively.

In Fig. 9 some examples of measured angular parts of the H(2p) electron cloud are displayed. As can be seen,

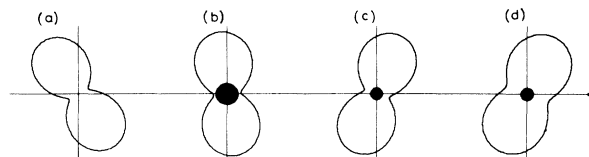


FIG. 9. Measured angular parts of H(2p) electron clouds in (a) 1-keV, (b) 1.5-keV, (c) 3-keV, and (d) 4-keV H⁺-He collisions ($b \approx 0.7$ a.u.). Shaded areas indicate size of circular polarization.

the electron clouds are in general aligned with an angle γ with respect to the internuclear axis. (For the scattering angles of typically a few degrees considered here this axis practically coincides with the z axis.) Moreover, this alignment angle γ depends on both the impact parameter b and the incident energy E . The electron clouds in Fig. 9, for example, have been obtained at an impact parameter $b \approx 0.7$ a.u. and for incident energies of 1, 1.5, 3, and 4 keV. While at 1 keV the electron cloud is aligned at an angle $\gamma = 121^\circ$, the alignment angle changes to about 67° at 4 keV. Qualitatively, this result is in agreement with observations by Andersen *et al.*¹⁴ for Li(2p) excitation in Li⁺-He collisions. As was pointed out by Kimura and Lane,²² this variation of the alignment angle γ arises from the passage of the relative phase χ between the excitation amplitudes f_{+1} and f_0 through π , which is due to the long-range π - π radial coupling between the two near-degenerate channels which correlate to Li(2p)+He⁺ and Li⁺+He(2¹P). The situation is similar for the H⁺-He collision system investigated here, and the same arguments may apply.

The measured values for the orientation $i\langle T(1)_{11} \rangle / \langle T(1)_{00} \rangle$ are summarized in Fig. 10. They are compared with recent theoretical calculations of Kimura and Lin.⁷ Magnitude and impact-parameter dependence of the orientation are well described by these calculations. In contrast, from *one-electron* model calcu-

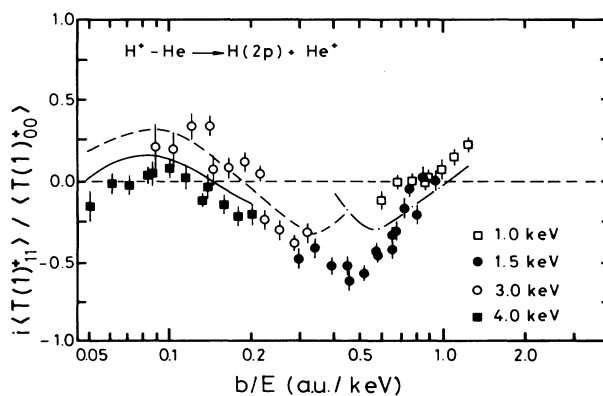


FIG. 10. Relative orientation vector $i\langle T(1)_{11} \rangle / \langle T(1)_{00} \rangle$ vs impact parameter b for 1 (□), 1.5 (●), 3 (○), and 4 (■)-keV H⁺-He collisions. Also shown are theoretical calculations by Kimura and Lin (Ref. 7) for 1 keV (dashed-dotted line), 3 keV (dashed line), and 4 keV (solid line).

lations of Fritsch¹⁸ one would expect a positive and too large $i\langle T(1)_{11}\rangle/\langle T(1)_{00}\rangle$, in disagreement with the experimental data. Obviously, the orientation is sensitive to finer details of the model and approximation used, and a *two-electron* description as used by Kimura and Lin appears to be essential here.

It should be noted here that the orientation and hence the transferred angular momentum component $\langle L_y \rangle$ is not a monotonous increasing or decreasing function of the impact parameter. In contrast to a simple "bouncing-ball" model, the indicated oscillating behavior is again due to a variation of the relative phase χ between the amplitudes f_{+1} and f_0 . We obtain the phase χ from $\langle T(1)_{11}\rangle$ and $\langle T(1)_{21}\rangle$, using

$$\tan\chi = -i\langle T(1)_{11}\rangle/\langle T(1)_{21}\rangle. \quad (6)$$

Here χ represents some average phase due to the fact that the total polarization $P < 1$. Some values for χ thus derived for $b \approx 0.7$ a.u. and as a function of incident energy E are displayed in Fig. 11. The relative phase $\chi = \chi_{+1} - \chi_0$ arises from different sources. One source is the development of the adiabatic phase $(-i/\hbar) \int E(R)dt$, which is different for χ_{+1} and χ_0 due to the different binding energies $E(R)$ of the MO states along which the amplitudes f_{+1} and f_0 evolve. As the collision time decreases with increasing collision energy, the contribution from this source decreases with $1/v$ (v being the projectile velocity). Using molecular energies calculated by Macias *et al.*²³ we estimate the corresponding phase difference to amount to about 145° and 73° for 1 and 4 keV incident energy, respectively. Other sources are associated with a phase change resulting from the passage of an avoided crossing, for example $2s\sigma-2p\sigma$ or the long-range $2p\pi-3d\pi$ coupling,^{11,24,25} and with the decoupling of electronic angular momenta from the internuclear axis.^{20,21}

In conclusion, we have presented a detailed experimental investigation of $H(2p)$ production in 1–4-keV H^+ -He collisions. Our results demonstrate the significance of the $2s\sigma-2p\sigma$ radial coupling in such asymmetric collisions. Not so well understood is the behavior of the relative phase χ between the excitation am-

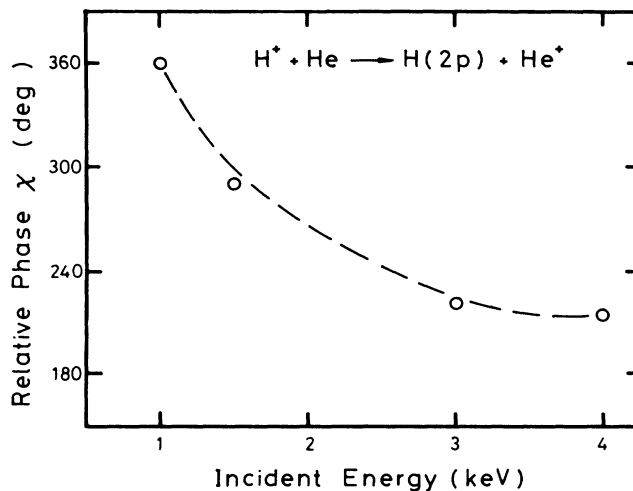


FIG. 11. Relative phase χ vs incident energy for $b \approx 0.7$ a.u. The dashed line is to guide the eye only.

plitudes f_1 and f_0 , which is complicated by the many different couplings along which the excitation process proceeds. As a result, simple propensity rules which crystallize the essence of the collision dynamics cannot be given yet. However, we are now studying in much the same way similar systems, for example, H-He. Hopefully, the systematics of such data will finally allow us to extract a rather complete and clear picture of these very basic collision systems.

ACKNOWLEDGMENTS

The authors acknowledge helpful discussions with Dr. W. Fritsch, Dr. M. Kimura, Professor C.-D. Lin, W. Harbich, and H. Madeheim. One of us (H.K.) would like to thank the Deutsche Forschungsgemeinschaft (DFG) and the University of Bielefeld for support and hospitality during his visits. The work was supported by the Deutsche Forschungsgemeinschaft (DFG) in Sonderforschungsbereich 216 "Polarisation und Korrelation in atomaren Stosskomplexen."

*Present address: II. Institut für Experimentalphysik, Universität Hamburg, 2000 Hamburg 50, Federal Republic of Germany.

†Permanent address: Atomic Physics Laboratory, University of Stirling, Stirling FK9 4LA, Scotland.

¹R. Hippler, G. Malunat, M. Faust, H. Kleinpoppen, and H. O. Lutz, *Z. Phys. A* **304**, 63 (1982).

²R. Hippler, M. Faust, R. Wolf, H. Kleinpoppen, and H. O. Lutz, *Phys. Rev. A* **31**, 1399 (1985).

³H. W. Hermann and I. V. Hertel, *Comments At. Mol. Phys.* **12**, 61 and 121 (1982).

⁴K. Blum and H. Kleinpoppen, *Phys. Rep.* **52**, 203 (1979); **96**, 251 (1983).

⁵R. Hippler, in *Fundamental Processes in Atomic Collision Physics*, edited by H. Kleinpoppen, J. S. Briggs, and H. O. Lutz (Plenum, New York, 1985), p. 181.

⁶M. Kimura and C. D. Lin, *Phys. Rev. A* **34**, 176 (1986).

⁷M. Kimura and C. D. Lin, *Abstracts of the Tenth International Conference on Atomic Physics*, Tokyo, 1986, edited by H. Narumi and I. Shimamura (North-Holland, Amsterdam, 1987), p. 487.

⁸U. Fano and J. Macek, *Rev. Mod. Phys.* **45**, 553 (1973).

⁹M. Born and E. Wolf, *Principles of Optics* (Pergamon, Oxford, 1980).

¹⁰N. Andersen, T. Andersen, J. O. Olsen, and E. Horsdal Pedersen, *J. Phys. B* **13**, 2421 (1980).

¹¹D. Mueller and D. H. Jaecks, *Phys. Rev. A* **32**, 2650 (1985).

¹²R. Hippler, W. Harbich, H. Madeheim, H. Kleinpoppen, and H. O. Lutz, *Phys. Rev. A* **35**, 3139 (1987).

¹³D. Doweck, Ph.D. thesis, Université de Paris-Sud, Orsay, 1983; D. Doweck, D. Dhuicq, V. Sidis, and M. Barat, *Phys. Rev. A* **26**, 746 (1982).

- ¹⁴N. Andersen, T. Andersen, H.-P. Neitzke, and E. Horsdal Pedersen, *J. Phys. B* **18**, 2247 (1985).
- ¹⁵J. Fayeton, J. C. Houver, M. Barat, and F. Masnou-Seeuws, *J. Phys. B* **9**, 461 (1976).
- ¹⁶M. Abignoli, M. Barat, J. Baudon, J. Fayeton, and J. C. Houver, *J. Phys.* **5**, 1533 (1972).
- ¹⁷J. Macek and C. Wang, *Phys. Rev. A* **34**, 1787 (1986).
- ¹⁸W. Fritsch (private communication).
- ¹⁹R. Hippler, W. Harbich, M. Faust, H. Kleinpoppen, H. O. Lutz, and L. Dubé, *J. Phys. B* **19**, 1507 (1986).
- ²⁰J. Grosser, *J. Phys. B* **14**, 1449 (1981).
- ²¹J. Grosser, *Z. Phys. D* **3**, 39 (1986).
- ²²M. Kimura and N. F. Lane, *Phys. Rev. Lett.* **56**, 2160 (1986).
- ²³A. Macias, A. Riera, and M. Yanez, *Phys. Rev. A* **23**, 2941 (1981); **27**, 206 (1983); **27**, 213 (1983).
- ²⁴V. A. Ankudinov, S. V. Bobashev, and V. I. Perel [*Zh. Eksp. Teor. Fiz* **60**, 906 (1971)] [*Sov. Phys.—JETP* **33**, 490 (1971)].
- ²⁵A. Russek, D. B. Kimball, and M. J. Cavagnero, *Phys. Rev. A* **23**, 139 (1981).